AGU PUBLICATIONS

Water Resources Research

TECHNICAL REPORTS: METHODS

10.1002/2017WR021496

Key Points:
- Repeated temperature-depth profiles provide an excellent opportunity to study the transience of subsurface heat flow processes
- The classic approach to infer ground water flow from temperature-depth profiles disturbed by surface warming has serious shortcomings
- Novel analytical approaches provide good estimates of groundwater flow when used on repeated temperature-depth profiles

Supporting Information:
- Supporting Information S1
- Data Set S1

Correspondence to:
V. F. Bense,
victor.bense@wur.nl

Citation:
Bense, V. F., Kurylyk, B. L., van Daal, J., van der Ploeg, M. J., & Carey, S. K. (2017). Interpreting repeated temperature-depth profiles for groundwater flow. *Water Resources Research*, *53*, 8639–8647. https://doi.org/10.1002/2017WR021496

Received 11 JUL 2017
Accepted 19 SEP 2017
Accepted article online 27 SEP 2017
Published online 27 OCT 2017

Interpreting Repeated Temperature-Depth Profiles for Groundwater Flow

Victor F. Bense[1], Barret L. Kurylyk[2,3], Jonathan van Daal[1], Martine J. van der Ploeg[1], and Sean K. Carey[2]

[1]Department of Environmental Sciences, Wageningen University and Research, Wageningen, The Netherlands, [2]School of Geography and Earth Sciences, McMaster University, Hamilton, ON, Canada, [3]Department of Civil and Resource Engineering Dalhousie University, Halifax, NS, Canada

Abstract Temperature can be used to trace groundwater flows due to thermal disturbances of subsurface advection. Prior hydrogeological studies that have used temperature-depth profiles to estimate vertical groundwater fluxes have either ignored the influence of climate change by employing steady-state analytical solutions or applied transient techniques to study temperature-depth profiles recorded at only a single point in time. Transient analyses of a single profile are predicated on the accurate determination of an unknown profile at some time in the past to form the initial condition. In this study, we use both analytical solutions and a numerical model to demonstrate that boreholes with temperature-depth profiles recorded at multiple times can be analyzed to either overcome the uncertainty associated with estimating unknown initial conditions or to form an additional check for the profile fitting. We further illustrate that the common approach of assuming a linear initial temperature-depth profile can result in significant errors for groundwater flux estimates. Profiles obtained from a borehole in the Veluwe area, Netherlands in both 1978 and 2016 are analyzed for an illustrative example. Since many temperature-depth profiles were collected in the late 1970s and 1980s, these previously profiled boreholes represent a significant and underexploited opportunity to obtain repeat measurements that can be used for similar analyses at other sites around the world.

1. Introduction

In the present warming climate, the Earth's continental land mass and oceans are sinks for heat (Beltrami et al., 2006), and subsurface temperature-depth (TD) profiles in the shallow crust (e.g., 50–200 m) indicate that thermal gradients are reversed from deeper positive gradients controlled by upward geothermal heat flow (e.g., Bodri & Cermak, 2007). Regional geological processes that control the rates of deep geothermal heat flow operate on geologic time scales, but heat flow from the surface into the crust is primarily controlled by variations in ground surface temperature (GST) due to changes in land use, atmospheric temperatures, or near-surface hydrology (Huang et al., 2009). In areas of significant regional groundwater flow, which typically occurs in sedimentary basins, the advection of heat by groundwater movement is a significant component of total heat flow, and thus heat can be employed as a tracer for relatively deep groundwater flow (Saar, 2011). However, if the thermal effects of groundwater flow are negligible, the propagation of higher-frequency GST changes into the crust is primarily driven by heat conduction, the rates of which are controlled by the thermal diffusivity and the nature of the GST variations due to climate change or urbanization (e.g., Bayer et al., 2016; González-Rouco et al., 2009). In these areas, relatively deep TD profiles (e.g., >500 m) have been analyzed with numerical inversion codes to reproduce a preobservational GST history by matching the observed transient signals in the TD profile (Smerdon & Pollack, 2016).

To quantitatively interpret transient TD profiles that are impacted by multiple heat flow processes, analytical forward solutions have been proposed to governing equations that consider heat transfer processes other than conduction (Carslaw & Jaeger, 1959; Taniguchi et al., 1999a, 1999b). These solutions can incorporate the thermal effects of vertical groundwater flow and have been developed with transient boundary conditions representing various scenarios of GST change over time. For example, a solution with a periodic boundary condition is commonly applied to trace groundwater from the downward propagation of diel (Rau et al., 2014) or seasonal (Kikuchi & Ferré, 2016; Stallman, 1965) GST variations. Alternatively, the GST boundary condition can represent the impact of long-term changes in climate or land cover by ignoring

high-frequency changes and considering only changes to mean annual GST (Taniguchi et al., 1999b). These low-frequency GST changes, which are the focus of this study, propagate more deeply than high-frequency changes. In principle, groundwater flow rates, rates of past surface warming, or both can be inferred from TD profiles (Kurylyk & MacQuarrie, 2014) by finding a best-fit of the forward model to field observations.

The application of a specific analytical solution to interpret TD profiles is relatively straight-forward. Few specific choices are made as each analytical solution can only be derived for a specific set of assumptions and has limited parameters. Two common and important assumptions are homogeneous thermal properties and uniform groundwater flow. The simplest analytical approach is a steady state analysis, which neglects the influence of climate change on subsurface temperature. Such an approach was first proposed by Bredehoeft and Papadopulos (1965) who provided a simple steady state solution that has been applied at many sites around the world to estimate vertical groundwater fluxes. When multidecadal transient heat flow is considered, an initial (at $t = 0$) TD profile at some point in the past is perturbed using GST changes to form the transient boundary condition (Anderson, 2005). If the TD profile is only available at one relatively recent point in time, transient analysis is predicated on assumed prior initial conditions, which can add considerable uncertainty in the analysis (Kurylyk & MacQuarrie, 2014; Taniguchi et al., 1999b). The specific mathematical function chosen to represent the initial conditions will influence the form of the analytical solution. It is, therefore, critical that the assumptions made at this stage do not violate the basic physical principles of the system under consideration, limiting the application of the solution. Taniguchi et al. (1999a) modified earlier analytical solutions (Carslaw & Jaeger, 1959) to interpret TD profiles influenced by the effects of groundwater flow and temporal changes in GST. These equations, herein identified as the CJT-methodology (in reference to Carslaw & Jaeger (1959) and Taniguchi et al. (1999a)) use linear functions for the initial and boundary conditions and have been applied extensively to analyze TD profiles impacted by past groundwater flow and surface warming (e.g., Miyakoshi et al., 2003; Taniguchi, 2006; Taniguchi et al., 2003; Taniguchi & Uemura, 2005; Uchida et al., 2003; Uchida & Hayashi, 2005) or applied to forward model the influence of future climate change on groundwater temperature (Gunawardhana et al., 2011; Gunawardhana & Kazama, 2011).

An alternative approach to interpret TD profiles is to utilize numerical models of subsurface heat flow to approximate solutions to the applicable heat flow equations. An important advantage of numerical models over analytical solutions is that flexibility exists in the representation of model elements such as boundary conditions, heterogeneity in hydraulic and thermal properties, and consideration of the multidimensionality of fluid and heat-fluxes (Bense & Beltrami, 2007; Bense & Kooi, 2004; Irvine et al., 2016). For simple scenarios, numerical solutions can also be compared to relatively simple analytical solutions for consistency among solution methods.

In this study, we analyze a TD profile recorded in the same borehole (Veluwe area, Netherlands) in 1978 and 2016 to revisit the applicability of the CJT-methodology and other techniques to interpret transient TD profiles in hydrogeologically active locations. Specifically, we test whether the linear initial conditions invoked in the commonly applied CJT-methodology can strongly influence the solution of the inverse problem to estimate groundwater fluxes from a TD profile. The evolution of the TD profile between 1978 and 2016 is also analyzed to examine whether repeat TD measurements can be applied to overcome the uncertainty associated with assuming unknown initial conditions when the TD profile is only available at one point in time. These questions are investigated by comparing the CJT-methodology to results from an alternative analytical solution that allows for nonlinear initial conditions (Kurylyk & Irvine, 2016) as well as simulations using a finite element model of groundwater flow and energy transfer.

2. Interpreting Repeated Temperature-Depth Profiles From the Deelen Site, Netherlands

In the autumn of 2016, TD data were obtained in 29 boreholes across the Veluwe area, Netherlands. Many of these had been previously logged in 1978. From an inspection of the 1978–82 data, it is clear that the temperature precision of the thermometer used was in the order of 10^{-2} °C; however, details on calibration controlling absolute accuracy are missing. These historic data were collected at 1 m depth intervals. In 2016, data were collected using a RBR soloT instrument (http://rbr-global.com) which was calibrated to an

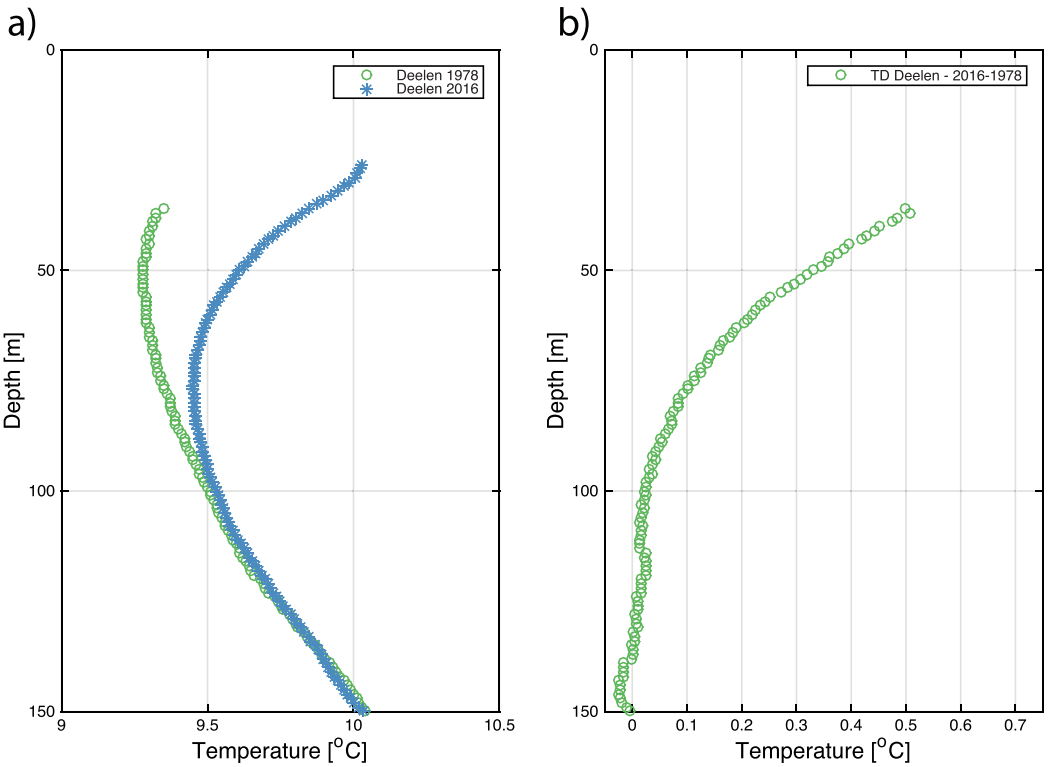

Figure 1. (a) Temperature-depth (TD) data for the Deelen site, Netherlands, obtained in 1978 (green circles) and 2016 (blue circles), (b) a "reduced" TD profile for the Deelen site obtained by subtracting the 1978 data from the 2016 TD profile. This quantifies the amount of subsurface warming and its distribution with depth occurring from 1978 to 2016.

accuracy of $\pm 1{\cdot}10^{-3}$ °C and has a temperature resolution of $<5{\cdot}10^{-6}$ °C and a time-constant of 1 s. For the 2016 data collection, the stop-go principle (Harris & Chapman, 2007) was used to collect temperature measurements each second for 10 s at each 1 m depth interval.

One set of repeated TD profiles, namely from the Deelen site (Figure 1), was analyzed in this study. This borehole is situated ($52^\circ 2' 39.98'' N / 5^\circ 54' 8.14'' E$) in a groundwater recharge area and is characterized by a relatively homogeneous subsurface consisting of loosely consolidated fine-medium grained sands. In this area, environmental tracers and hydrogeological modeling suggest that groundwater recharge is in the order of 0.35 $m{\cdot}a^{-1}$ (Gehrels, 1999).

The distinct C-shape of the TD profile that is indicative of transient conditions resulting from recent surface warming is clearly present in 1978 (Figure 1a), suggesting surface warming at this location began some time before 1978. Moreover, the increased curvature by 2016 implies that surface warming persisted after 1978. At the base of the profile ($z = 150$ m) the temperature gradient (0.012 °C · m^{-1}) remained constant over the time period within the precision and accuracy of the temperature measurements. By assuming a standard thermal conductivity (κ) for sandy sediments of 2.7 $W{\cdot}m^{-1}$ °C^{-1}, we estimated the background heat flow density at this depth to be $32{\cdot}10^{-3}$ $W{\cdot}m^{-2}$. The depth-point at which $\frac{\partial T}{\partial z} = 0$ (known as the "inflection point") has migrated by 23 m, i.e., from $z = 53$ to $z = 76$ m, between 1978 and 2016. Herein our analysis is not restricted to the inflection point but rather considers the entire TD profile. By employing this approach, we can compare results from standard techniques (Taniguchi et al., 1999b) to those found from a new, flexible analytical solution (Kurylyk & Irvine, 2016), and a numerical model (FlexPDE), which is described below.

2.1. Methodology

All discussed model simulations rely on solutions of the transient conduction-advection heat-flow equation in the Cartesian *z*-direction (depth) (Stallman, 1965):

$$\kappa \frac{\partial^2 T}{\partial z^2} - c_w \rho_w \frac{\partial (q_z T)}{\partial z} = c_b \rho_b \frac{\partial T}{\partial t} \quad (1)$$

where T (°C) is temperature, t (s) is time, κ (W·m^{-1}·°C^{-1}) is the thermal conductivity, q_z (m· a^{-1}) is the z-component of specific discharge, c_w and c_0 (J·kg^{-1}·°C^{-1}) are, respectively, the specific heat of fluid and solid–fluid medium, and ρ_w and ρ_0 (kg·m^{-3}) represent the density of the water and medium, respectively.

Figure 2 schematically shows the system that is being described by equation (1), and the boundary conditions (BCs) that are required to condition a solution to equation (1). GST was not recorded on site, yet GST and surface air temperature (SAT), of which there are records available (http://knmi.nl) that are representative of the Veluwe region as a whole (Figure 2b), are usually strongly coupled (Smerdon & Pollack, 2016). Hence, we prescribed the surface temperature boundary condition (T_s) using the SAT but allowed for a constant temperature offset between them. The initial surface temperature (T_0) should in principle be the average GST prior to when surface warming started and is used to calculate a TD profile at $t = 0$ representing a steady state situation that would have existed prior to when surface warming started. Here, we used the year 1965 as $t = 0$ because that is approximately when the meteorological record starts to indicate sustained atmospheric warming. We did not investigate the impact on groundwater flux estimates of considering different times for $t = 0$. The offset between GST and SAT can be determined in practice by finding values for the GST at $t = 0$. We found that we needed different values for T_0 for each methodology to obtain good fits between observed (1978 and 2016) and modeled TD profiles. Furthermore, we consider that simple approaches to find T_0 that for instance linearly extrapolate the portion of the TD profile that is undisturbed by surface warming (e.g., >100 m depth) to the land surface (e.g., Bayer et al., 2016; Gunawardhana et al., 2011) might not yield good results in areas of relatively strong groundwater flow. This is because such approach does not consider the curvature of the TD profile in such situation as it would have existed at $t = 0$. Also for each method, we had to use a different representation of the climate record to form the surface boundary condition (e.g., linear warming versus step changes, Figure 2) given the differences in the

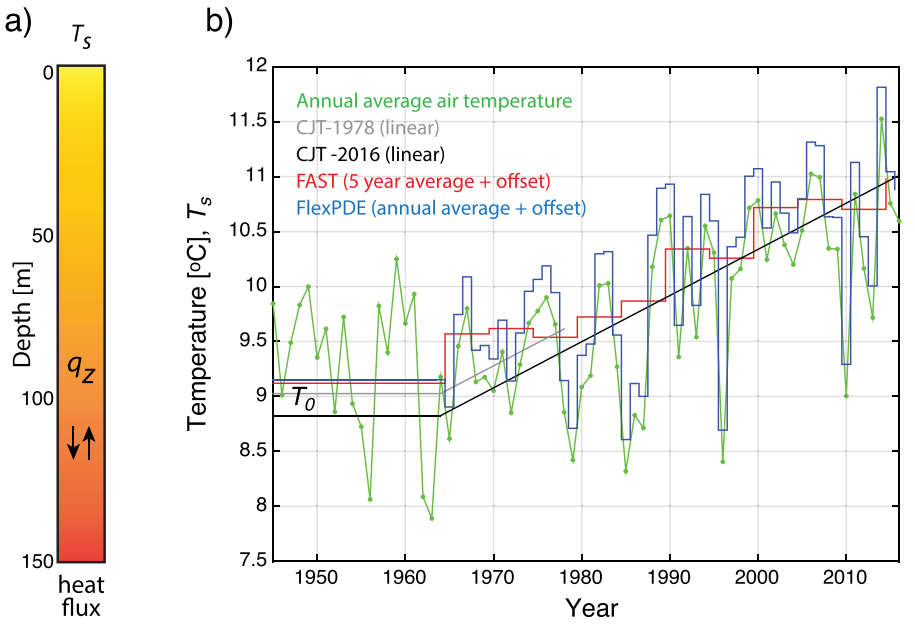

Figure 2. (a) Conceptual representation of the system modeled using the three methodologies applied here. The thermal boundary conditions to the system include a background temperature gradient (T_G (°C· m^{-1})) at the base indicative of geothermal heat flow, as well as the ground surface temperature (T_s (°C)) at the surface. The latter is represented in various different ways (b) in the modeling codes (e.g., step functions or linear warming rates), but is always based a time averaging of the measured air temperature record with an offset to obtain surface temperature (see text for discussion). All simulations start in 1965, and for the IC representing the period prior to 1965 various different T_0 were chosen for each model (Table 1), so that a satisfactory fit is obtained between modeled TD profiles and those observed at the Deelen site in 1978 and 2016.

mathematical nature of the boundary condition functions as detailed below. Subsurface thermal properties were selected based on standard values that have been used in previous heat flow studies focusing on the Netherlands (Bense & Kooi, 2004; Kooi, 2008): $\kappa = 2.7$ W·m^{-1} °C^{-1}; $c_w\rho_w = 4.18{\cdot}10^6$ J·m^{-3}·°C^{-1}; and $c_b\rho_b = 4.15{\cdot}10^6$ J·m^{-3}·°C^{-1}.

2.1.1. Carslaw-Jaeger-Taniguchi (CJT)

For a linear increase in GST, Carslaw and Jaeger (1959) derived an analytical solution to equation (1), describing the time-evolution of a TD profile as (Taniguchi et al., 1999a):

$$\begin{aligned} T(z,t) &= T_0 + T_G(z-Ut) + (b+T_G U)/2U \\ &\cdot[(z+UT)e^{Uz/\alpha}\mathrm{erfc}(z+Ut)/\left(2\sqrt{\alpha t}\right) \\ &+ (Ut-z)\mathrm{erfc}(z-Ut)/\left(2\sqrt{\alpha t}\right)] \end{aligned} \tag{2}$$

in which $\alpha = \frac{\kappa}{c_b\rho_b}$ (m$^2 \cdot s^{-1}$) is the thermal diffusivity, and $U = q_z \frac{c_0\rho_0}{c_b\rho_b}$. Equation (2) is valid for a linear initial ($t = 0$) TD profile:

$$T(z, t=0) = T_0 + (T_G \cdot z) \tag{3}$$

where T_0 is the GST at $t = 0$, and T_G (°C·m^{-1}] is the background thermal gradient. As previously noted, this initial condition implies that at $t = 0$, $q_z = 0$ as curvature in the TD profile would otherwise exist (Bredehoeft & Papadopulos, 1965).

The boundary condition for equation (2) represents a mean annual GST that is warming at a linear rate:

$$T(z=0, t) = T_0 + (b \cdot t) \tag{4}$$

where b (°C·a^{-1}) is the rate of increase in mean annual GST.

Given the deep undisturbed geothermal gradient (T_G) in the measured TD profiles (Figure 1) as well as the other parameterization described above, only T_0 and q_z were unknowns when applying the CJT methodology to obtain a fit to the two Deelen TD profiles. For both cases, a linear 1965 profile was used to form the initial conditions.

2.1.2. FAST

The FAST (Flexible Analytical Solution using Temperature) model is written in the Python computing language and incorporates a new analytical solution with nonlinear initial conditions and flexible boundary conditions (Irvine et al., 2017; Kurylyk & Irvine, 2016) to accommodate TD profile curvature due to prior climate change and/or groundwater flow (Kurylyk & Irvine, 2016).

$$T(z, t=0) = T_i + T_G \cdot z + \delta e^{(dz)} \tag{5}$$

where $T_i + \delta = T_0$ and d (m^{-1}) can be adjusted to create curvature in the initial profile. The parameters in this function can be adjusted so that the resultant semi-infinite TD profile matches the profile produced by the classic analytical solution derived by Bredehoeft and Papadopulos (1965) for a steady state TD profile influenced by advection. The Bredehoeft and Papadopulos (1965) equation cannot be applied directly to form the initial condition as this is only a finite solution, and the analytical solution (equation (7)) is derived for a semi-infinite domain similar to the solution by Taniguchi et al., (1999a).

The boundary condition is formed by any number of superimposed step changes and can represent complex intermittent warming and cooling trends (Menberg et al., 2014):

$$T(z=0, t) = \sum_{j=1}^{n} (T_0 + \Delta T_j \times H(t - t_j)) \tag{6}$$

where T_j (°C) is the change in surface temperature at the jth step, and t_j (s) is the time as $t = 0$ to the beginning of step j. H is the Heaviside function that turns the steps on at the appropriate times. The FAST model

allows the user to quickly process climate data to form the multistep boundary condition and forward model the initial conditions using the resultant analytical solution as:

$$T(z,t)=T_G z+T_i-UT_G t+\delta\exp\left(\alpha d^2 t+dz-Udt\right)+$$
$$\frac{T_0-T_i}{2}\left[\operatorname{erfc}\left(\frac{z-Ut}{2\sqrt{\alpha t}}\right)+\exp\left(\frac{Uz}{\alpha}\right)\operatorname{erfc}\left(\frac{z+Ut}{2\sqrt{\alpha t}}\right)\right]+$$
$$\sum_{j=1}^{n}\left\{\frac{\Delta T_j}{2}\left[\operatorname{erfc}\left(\frac{z-U(t-t_j)}{2\sqrt{\alpha(t-t_j)}}\right)+\exp\left(\frac{Uz}{\alpha}\right)\operatorname{erfc}\left(\frac{z+U(t-t_j)}{2\sqrt{\alpha(t-t_j)}}\right)\right]H(t-t_j)\right\}+$$
$$\frac{T_G}{2}\left\{(Ut-z)\operatorname{erfc}\left(\frac{z-Ut}{2\sqrt{\alpha t}}\right)+(Ut+z)\exp\left(\frac{Uz}{\alpha}\right)\operatorname{erfc}\left(\frac{z+Ut}{2\sqrt{\alpha t}}\right)\right\}- \tag{7}$$
$$\frac{\delta}{2}\exp\left\{\frac{Uz}{2\alpha}+\alpha d^2 t-Udt\right\}\left\{\exp\left(-z\sqrt{\frac{U^2}{4\alpha^2}+d^2-\frac{Ud}{\alpha}}\right)\operatorname{erfc}\left(\frac{z}{2\sqrt{\alpha t}}-\sqrt{\frac{U^2 t}{4\alpha}+\alpha d^2 t-Udt}\right)+\right.$$
$$\left.\exp\left(z\sqrt{\frac{U^2}{4\alpha^2}+d^2-\frac{Ud}{\alpha}}\right)\operatorname{erfc}\left(\frac{z}{2\sqrt{\alpha t}}+\sqrt{\frac{U^2 t}{4\alpha}+\alpha d^2 t-Udt}\right)\right\}$$

For FAST, a 1965 steady state profile was generated fitting the deeper part of the observed profile not showing any change between 1978 and 2016 (i.e., below $z = 110$ m; Figure 1b) using the Bredehoeft and Papadopulos (1965) (BP) solution. BP requires temperatures to be specified at the top and bottom of the profile. The bottom temperature was obtained from the undisturbed portion of the profile, and the upper temperature ($T_0 = 9.12$°C) was obtained by averaging the climate data before 1965. The optimal BP fit to the lower part of the profile was found for a q_z of 0.30 m·a^{-1}. An excellent fit (RMSE = 5·10^{-5}°C) to the BP profile between 0 and 150 m was obtained using equation (6), and this fit was applied as the initial condition for FAST. This profile was forward modeled using the transient boundary condition (Figure 2b) constructed by fitting the climate data with the multistep function with 5 year intervals to smooth out high-frequency variability (Ferguson & Woodbury, 2004). An optimal Darcy flux was obtained by manually adjusting the Darcy flux until the RMSE between the measured and calculated 2016 profiles was minimized.

2.1.3. Numerical Modeling: FlexPDE

In addition to the two analytical techniques described above, we applied a numerical code, FlexPDE, to simulate the Deelen data set. FlexPDE is a flexible numerical modeling environment based upon the finite-element method to solve partial differential equations such as equation (1). FlexPDE was tested successfully against benchmark problems and used in several earlier studies to describe heat-flow in hydrogeological systems (e.g., Bense & Beltrami, 2007).

For the numerical model based upon FlexPDE, we simulated a steady state TD profile representing the 1965 situation, using a combination of T_0 and q_z that resulted in a good fit, with minimal RMSE, between the model and the deeper part of the observed profile not showing any change between 1978 and 2016 (i.e., below $z = 110$ m; Figure 1b). The offset between T_s that was found for 1965 was then maintained as an offset for the observed annual air temperature record which was applied as the GST boundary condition using the annual averages (Figure 2b). As shown in Figure 2a, heat flow in FlexPDE is driven by an up flow of heat from the deeper crust and is assigned as a boundary condition at the bottom of the domain (Neumann-type BC). A thermal gradient (T_G) at the base is used which implies a heat flow boundary. At the surface, a specified temperature (T_s (°C)) is assigned (Dirichlet-type BC) to represent the GST (Figure 2b).

Note that all of the numerical and analytical approaches described in this text assume uniform vertical groundwater flux, but the vertical component of flux often decreases with depth. We have invoked this assumption to be consistent among all methods and to focus on the influence of the initial conditions. Others have investigated this uniform flux assumption in more detail, and have generally shown that these methods produce the average vertical component of the flux even when it varies with depth (Irvine et al., 2016).

3. Results and Discussion

The three methodologies were applied independently to obtain a model fit to the TD profiles of the Deelen data set (Figure 1). The vertical groundwater fluxes inferred from the application of the three applied

Table 1
Inferred q_z for the Deelen TD Data Set Using the CJT, FAST and FlexPDE Approach Using Variations in BC/IC

	CJT			
	q_z (m·a^{-1})	RMSE (°C)	T_0 (pre-1965)	T_G (°C·m^{-1})
2016	0.675	0.021	8.82	0.010
1978	3.4	0.037	9.03	0.010
1965	0	0.51/0.31	9.03/8.82	0.010
	FAST			
2016	0.300	0.020	9.12	0.014
1978	0.300	0.019	9.12	0.014
1965	0.300	0.016	9.12	0.014
	FlexPDE			
2016	0.400	0.022	9.17	0.010
1978	0.400	0.019	9.17	0.010
1965	0.400	0.016	9.17	0.010

Note. The root-mean-square-error (RMSE) (°C) between field data and model prediction is given as $RMSE = \sqrt{\frac{1}{n}\sum_{i=1}^{n}(T_{model,i} - T_{observed,i})^2}$, and was calculated for the entire profile for 1978 and 2016, and from a depth of 75 m for the 1965 IC profile. The T_0 and T_G model parameters are also presented for each run. See text for discussion.

methodologies as well as the parameters that were used to obtain these fits are summarized in Table 1. The modeled TD profiles are all shown with the field data in Figure 3.

Figure 3 indicates that the FAST and FlexPDE methodologies yield similar results both in terms of goodness of fit (low RMSE values) and plausibility of the inferred vertical groundwater flux. For both methods, we obtain a downward groundwater velocity (0.3 and 0.4 m·a^{-1} for FAST and FlexPDE, respectively) that is in agreement with the expected groundwater flux at this location based on earlier studies (0.35 m·a^{-1}, Gehrels, 1999). One important feature of the FAST and FlexPDE models is that the same groundwater flux could be used to satisfactorily fit both the 1978 and 2016 TD profiles using the forcing generated by the imposed T_s record starting in 1965 from the same solution parameters and initial TD profile (1965). Thus, having two TD profiles temporally separated by several decades provides an additional check when using transient solutions to trace vertical groundwater fluxes. Additionally, when repeat TD profiles are available, the issue of an unknown initial condition can be overcome by using the first TD profile to form the initial condition for analyses conducted with either numerical or analytical techniques. As an example, the 1978 TD profile was applied as the initial condition for one FAST run forward modelled to 2016. The results (not shown) indicate a Darcy flux of 0.30 m/yr and agree with results obtained when the steady-state 1965 TD profile was applied as the initial condition (Figure 3b). We note that using either an annual average (FlexPDE) record of T_s, or a somewhat smoothed record using 5 year averages (FAST) does not result in notably different outcomes for this borehole. These set of features of both the FAST and FlexPDE runs indicate that these codes credibly represent the evolution of the subsurface regime at the Deelen site over the past 52 a. This is in contrast with the results obtained with the more commonly applied CJT model.

It was possible to iteratively obtain acceptable fits between the TD profiles calculated using the CJT model and the 1978 and 2016 field data (Figure 3a). However, these fits were only possible when using different values of T_0 and q_z when fitting either the 1978 or 2016 data (Table 1). Also, in both cases, the linear initial TD profile was significantly warmer (by several 0.1°C) than the observed TD profiles, even for depths (e.g., 150 m) at which the profile was presumably unchanged since 1965 (Figure 3a). Thus, it proved impossible

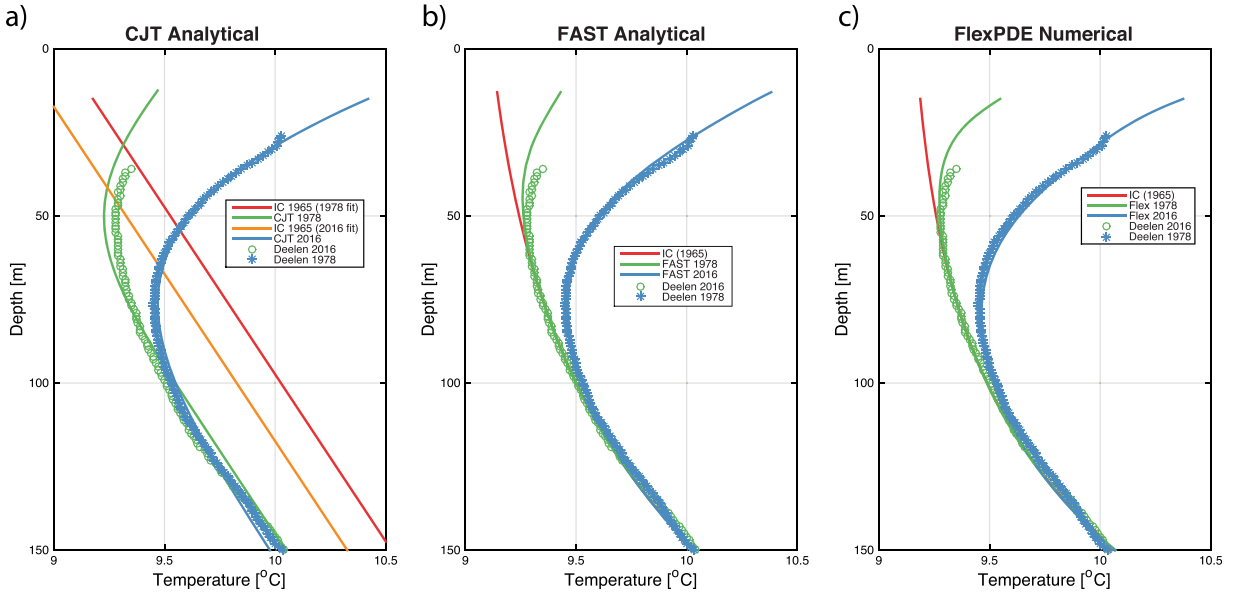

Figure 3. Model calculations (representing the initial model condition (IC) valid for 1965, and model predictions for 1978 and 2016) compared against TD field data from the Deelen site using (a) the analytical CJT-approach, (b) FAST, and (c) the numerical model FlexPDE.

to maintain a physical consistency between the 1978 and 2016 fits. Furthermore, although the fits themselves are reasonable (Figure 3a), the values for q_z inferred with the selected T_0 and T_G values, are unrealistic for the Deelen site. The value of q_z for 1978 is about 1 order of magnitude larger than is expected for the site, while the 2016 value is about two-times too large.

The underlying causes for the issues associated with the application of the CJT model are explained by an inspection of the linear initial profiles (1965) used for these model runs (Figure 3a). As a result of the assumption of q_z=0 at $t = 0$, the initial profile must quickly evolve in the periods between 1965 and 1978 or 2016. During this time period, the entire profile is either warming (for a scenario of groundwater seepage, not shown here) or cooling (for groundwater recharge, as at the Deelen site). Hence, the initial linear profile in this study required to obtain a fit to the 1978 or 2016 data is warmer by several 0.1°C than what is observed in 1965 (Figure 3a). Moreover, an unrealistically high q_z is imposed to generate sufficient curvature in the profile to match the 1978 data set at $t = 13$ a. A smaller q_z suffices when fitting the 2016 data as more time lapses from when the TD profile is linear at $t = 0$ in 1965 (i.e., $t = 51$ a).

From another perspective, the groundwater flux that is implicit in the initial conditions ($q_z = 0$) for the CJT approach is not in agreement with the groundwater flux that is explicit in the forward modeling (Table 1). This contradiction results in a TD profile that is offset even at great depths over time. For example, the observed TD profiles do not change considerably below 110 m between 1978 and 2016, but the CJT data exhibits extreme offsets between 1965 and 1978 or 2016 all the way down to 150 m (Figure 3a). Such offsets are also common in other studies even when forward modeling from a present-day initial condition with unreasonably high fluxes (Kurylyk & MacQuarrie, 2014), but, to our knowledge, they have not been previously explained. Both the FAST and FlexPDE results indicate that the profiles are not changing at great depths between 1965 and 2016 (Figures 3b and 3c). This is because the groundwater flux in the initial conditions (e.g., $q_z = 0.30$ m·a^{-1} for the initial conditions generated for FAST using the Bredehoeft & Papadopulos (1965) approach) matches the flux in the forward modeling in both cases.

4. Conclusions

The CJT methodology has been widely used (see references in the introduction) to interpret TD data that are impacted by groundwater flow and surface warming. However, such studies have relied on TD profiles obtained at single moments in time. Analyses of a repeated TD profile, taken 28 apart in the same borehole from a hydrogeologically active area, has illustrated shortcomings in the CJT methodology. In this study, we showed that its application to interpret repeated TD logs led to erroneous, and physically inconsistent results in estimating groundwater flow rates from TD profiles impacted by surface warming. This is mainly caused by simplifying assumptions for the shape and nature of the initial TD profile (at $t = 0$) that is taken as linear in the CJT approach. Alternative approaches, such as the recently developed analytical FAST model and numerical models, are more able to consistently interpret TD profiles.

Repeated TD logs represent a significant advancement in the use of heat as a groundwater tracer because such long-term data can accurately document the nature and magnitude of transience in subsurface heat flow described by transient models. In this study, we have specifically shown that repeat TD profiles can be used to either eliminate uncertainty associated with a typically unknown initial condition or to form an additional check in the transient modeling which can reveal errors in the underlying methodology. Several decades have passed since the intensive borehole temperature logging conducted in the 1970s and 1980s. Previously profiled boreholes in hydrogeologically active environments can be thermally logged to provide inexpensive and relatively robust estimates of vertical groundwater flux.

Acknowledgments
The water company Vitens is thanked for granting permission to carry out temperature measurements in groundwater observation boreholes that are part of their network. Ty Ferre and an anonymous reviever are thanked for constructive criticism that contributed to improve the quality of our original manuscript. TD data from the Deelen site and model results are available in tabulated form as supplementary information to this paper.

References

Anderson, M. (2005). Heat as a ground water tracer. *Ground Water*, *43*(6), 951–968. https://doi.org/10.1111/j.1745-6584.2005.00052.x

Bayer, P., Rivera, J. A., Schweizer, D., Schärli, U., Blum, P., & Rybach, L. (2016). Extracting past atmospheric warming and urban heating effects from borehole temperature profiles. *Geothermics*, *64*, 289–299. https://doi.org/10.1016/j.geothermics.2016.06.011

Beltrami, H., Bourlon, E., Kellman, L., & González-Rouco, J. F. (2006). Spatial patterns of ground heat gain in the northern hemisphere. *Geophysical Research Letters*, *33*, L06717. https://doi.org/10.1029/2006GL025676

Bense, V., & Beltrami, H. (2007). Impact of horizontal groundwater flow and localized deforestation on the development of shallow temperature anomalies. *Journal of Geophysical Research*, *112*, F04015. https://doi.org/10.1029/2006JF000703

Bense, V. F., & Kooi, H. (2004). Temporal and spatial variations of shallow subsurface temperature as a record of lateral variations in groundwater flow. *Journal of Geophysical Research*, *109*, B04103. https://doi.org/10.1029/2003JB002782

Bodri, L., & Cermak, V. (2007). *Borehole climatology: A new method how to reconstruct climate*. Amsterdam, the Netherlands: Elsevier Science.

Bredehoeft, J. D., & Papadopulos, I. S. (1965). Rates of vertical groundwater movement estimated from the Earth's thermal profile. *Water Resources Research*, *1*(2), 325–328.

Carslaw, H. S., & Jaeger, J. C. (1959). *Conduction of heat in solids* (2nd ed., 388 p.). Oxford, UK: Clarendon Press.

Ferguson, G., & Woodbury, A. D. (2004). Subsurface heat flow in an urban environment. *Journal of Geophysical Research*, *109*, B02402. https://doi.org/10.1029/2003JB002715

Gehrels, J. C. (1999). *Groundwater level fluctuations: Separation of natural from anthropogenic influences and determination of groundwater recharge in the Veluwe area, the Netherlands*. Amsterdam, the Netherlands: Vrije Universiteit.

González-Rouco, J. F., Beltrami, H., Zorita, E., & Stevens, M. B. (2009). Borehole climatology: A discussion based on contributions from climate modeling. *Climate of the Past Discussions*, *5*, 97–127.

Gunawardhana, L., & Kazama, S. (2011). Climate change impacts on groundwater temperature change in the Sendai plain, Japan. *Hydrological Processes*, *25*, 2665–2678. https://doi.org/10.1002/hyp.8008

Gunawardhana, L., Kazama, S., & Kawagoe, S. (2011). Impact of urbanization and climate change on aquifer thermal regimes. *Water Resources Management*, *25*, 3247–3276. https://doi.org/10.1007/s11269-011-9854-6

Harris, R. N., & Chapman, D. S. (2007). Stopgo temperature logging for precision applications. *Geophysics*, *72*(4), E119–E123.

Huang, S., Taniguchi, M., Yamano, M., & Wang, C-H. (2009). Detecting urbanization effects on surface and subsurface thermal environment: A case study of Osaka. *Science of the Total Environment*, *407*, 3142–3152.

Irvine, D. J., Cartwright, I., Post, V. E., Simmons, C. T., & Banks, E. W. (2016). Uncertainties in vertical groundwater fluxes from 1-d steady state heat transport analyses caused by heterogeneity, multidimensional flow, and climate change. *Water Resources Research*, *52*, 813–826. https://doi.org/10.1002/2015WR017702

Irvine, D. J., Kurylyk, B. L., Cartwright, I., Bonham, M., Post, V. E., Banks, E. W., & Simmons, C. T. (2017). Groundwater flow estimation using temperature-depth profiles in a complex environment and a changing climate. *Science of the Total Environment*, *574*, 272–281. https://doi.org/10.1016/j.scitotenv.2016.08.212

Kikuchi, C., & Ferré, T. (2016). Analysis of subsurface temperature data to quantify groundwater recharge rates in a closed altiplano basin, northern Chile. *Hydrogeology Journal*, *25*, 103–121. https://doi.org/10.1007/s10040-016-1472-1

Kooi, H. (2008). Spatial variability in subsurface warming over the last three decades; insight from repeated borehole temperature measurements in the Netherlands. *Earth and Planetary Science Letters*, *270*(1), 86–94.

Kurylyk, B. L., & Irvine, D. J. (2016). Analytical solution and computer program (FAST) to estimate fluid fluxes from subsurface temperature profiles. *Water Resources Research*, *52*, 725–733. https://doi.org/10.1002/2015WR017990

Kurylyk, B. L., & MacQuarrie, K. T. (2014). A new analytical solution for assessing climate change impacts on subsurface temperature. *Hydrological Processes*, *28*, 3161–3172. https://doi.org/10.1002/hyp.9861

Menberg, K., Blum, P., Kurylyk, B. L., & Bayer, P. (2014). Observed groundwater temperature response to recent climate change. *Hydrology and Earth System Sciences*, *18*, 4453–4466. https://doi.org/10.5194/hess-18-4453-2014

Miyakoshi, A., Uchida, Y., Sakura, Y., & Hayashi, T. (2003). Distribution of subsurface temperature in the Kanto Plain, Japan; estimation of regional groundwater flow system and surface warming. *Physics and Chemistry of the Earth*, *28*(9–11), 467–475. https://doi.org/10.1016/S1474-7065(03)00066-4

Rau, G. C., Andersen, M. S., McCallum, A. M., Roshan, H., & Acworth, I. (2014). Heat as a tracer to quantify water flow in near-surface sediments. *Earth-Science Reviews*, *129*, 40–58.

Saar, M. O. (2011). Review: Geothermal heat as a tracer of large-scale groundwater flow and as a means to determine permeability fields. *Hydrogeology Journal*, *19*(1), 31–52.

Smerdon, J. E., & Pollack, H. N. (2016). Reconstructing earth's surface temperature over the past 2000 years: The science behind the headlines. *Wiley Interdisciplinary Reviews: Climate Change*, *7*(5), 746–771.

Stallman, R. W. (1965). Steady one-dimensional fluid flow in a semi-infinite porous medium with sinusoidal surface temperature. *Journal of Geophysical Research*, *70*(12), 2821–2827.

Taniguchi, M. (2006). Anthropogenic effects on subsurface temperature in Bangkok. *Climate of the past Discussions*, *2*, 831–846.

Taniguchi, M., Shimada, J., Tanaka, T., Kayane, I., Sakura, Y., Shimano, Y., Dapaah-Siakwan, S., & Kawashima, S. (1999a). Disturbances of temperature-depth profiles due to surface climate change and subsurface water flow: 1. An effect of linear increase in surface temperature caused by global warming and urbanization in the Tokyo metropolitan area, japan. *Water Resources Research*, *35*(5), 1507–1517.

Taniguchi, M., Shimada, J., & Uemura, T. (2003). Transient effects of surface temperature and groundwater flow on subsurface temperature in Kumamoto plain, Japan. *Physics and Chemistry of the Earth, Parts A/B/C*, *28*(9–11), 477–486. https://doi.org/10.1016/S1474-7065(03)00067-6

Taniguchi, M., & Uemura, T. (2005). Effects of urbanization and groundwater flow on the subsurface temperature in Osaka, Japan. *Physics of the Earth and Planetary Interiors*, *152*, 305–313. https://doi.org/10.1016/j. pepi.2005.04.006

Taniguchi, M., Williamson, D. R., & Peck, A. J. (1999b). Disturbances of temperature-depth profiles due to surface climate change and subsurface water flow: 2. An effect of step increase in surface temperature caused by forest clearing in southwest western Australia. *Water Resources Research*, *35*(5), 1519–1529.

Uchida, Y., & Hayashi, T. (2005). Effects of hydrogeological and climate change on the subsurface thermal regime in the Sendai Plain. *Physics of the Earth and Planetary Interiors*, *152*, 292–304. https://doi.org/10.1016/j. pepi.2005.04.008

Uchida, Y., Sakura, Y., & Taniguchi, M. (2003). Shallow subsurface thermal regimes in major plains in japan with reference to recent surface warming. *Physics and Chemistry of the Earth, Parts A/B/C*, *28*(9–11), 457–466. https://doi.org/10.1016/S1474-7065(03)00065-2